

# THE MEASURING OF ETHER-DRIFT VELOCITY AND KINEMATIC ETHER VISCOSITY WITHIN OPTICAL WAVES BAND

**Yu.M. Galaev<sup>1</sup>**

*The Institute of Radiophysics and Electronics of NSA in Ukraine,  
12 Ac. Proskury St., Kharkov, 61085 Ukraine*

*Received November 15, 2002*

The experimental hypothesis verification of the ether existence in nature, i.e. the material medium, responsible for electromagnetic waves propagation has been performed. The optical measuring method of the ether movement velocity and the ether kinematic viscosity has been proposed and realized. The results of systematic measurements do not contradict the original hypothesis statements and can be considered as experimental imagination confirmation of the ether existence in nature, as the material medium.

The experimental hypothesis verification of the ether existence in nature, i.e. material medium, responsible for electromagnetic waves propagation has been performed earlier in the works [1-3], within millimeter radio waves band, by the phase method. The results of the experiment [1-3] do not contradict the original hypothesis statements, based on the ether model of V.A. Atsukovsky [4-6]. In the model [4-6] the ether is introduced by the material medium composed of separate particles, that fills in the world space, has the properties of viscous and coercible gas, is the construction material for all material formations. The physical fields represent the ether various movement forms, i.e. the ether is the material medium, responsible for electromagnetic waves propagation. The experimental model basis [4-6] was, first of all, the positive results of the ether drift search published by D.C. Miller in 1922-1926 [7-9] and A.A. Michelson, F.G. Pease and F. Pearson in 1929 [10].

The experiment [7-9] is performed within the electromagnetic waves optical band, differed by careful preparation, verified methods of the investigation conducting and statistically significant measurement results. The measured ether drift parameters mismatched to the ether imaginations available at that time, as stationary medium. Orbital component of the ether drift velocity, stipulated by the Earth movement around the Sun with the velocity 30 km/sec, was not detected. Miller obtained, that the ether drift velocity at the height of 265 m above the sea level (Cleveland, USA) has the value about 3 km/sec, and at the height of 1830 m (Mount Wilson observatory, USA) — about 10

km/sec. The apex coordinates the Solar system movement were determined: direct ascension  $\alpha \approx 17.5^h$ , declination  $\delta \approx +65^\circ$ . Such movement is almost perpendicular to an ecliptic plain (coordinates of the North Pole ecliptic:  $\alpha \approx 18^h$ ,  $\delta \approx +66^\circ$ ). Miller showed, that the observed effects can be explained, if to accept, that the ether stream has a galactic (space) origin and the velocity more than 200 km/sec. Almost perpendicularly directional orbital component of the velocity is lost on this background. Miller referred the velocity decrease of the ether drift from 200 km/sec up to 10 km/sec to unknown reasons.

Some peculiarities of the experiment results [7-9] and [10], are explained by the ether viscosity in the works [4-6]. In this case the boundary layer, in which the ether movement velocity (the ether drift) increases with the height growth above the Earth's surface, is formed at the relative movement of the solar System and the ether near the Earth's surface.

In the works [1-3] it is shown, that the results of systematic experimental investigations within radio waves band can be explained by the wave propagation phenomenon in the moving medium of a space origin with a vertical velocity gradient in this medium stream near the Earth's surface. The gradient layer availability can be explained by this medium viscosity, i.e. the feature proper to material media, the media composed of separate particles. The mean value of the measured maximal gradients was equal to 8.6 m/sec · m. The velocity comparison of the suspected ether drift, measured in the experiments [1-3], [7-9] and [10], is performed in the works [1-3]. The place distinctions of geographic latitudes and their heights above the sea level are taken

<sup>1</sup>e-mail: galaev@ire.kharkov.ua; Ph.: +38 (0572) 27-30-52

into account in these experiments conducting at comparison. It is obtained, that in the experiment [1-3] the ether drift velocity is within 6124...8490 m/sec, that according to the value order coincide with the data of the works [7-9] and [10], which are within 6000...10000 m/sec. The comparison result can be considered as mutual truthfulness confirmation of the experiments [1-3], [7-9] and [10].

The positive results of three experiments [1-3], [7-9], [10] give the basis to consider the effects detected in these experiments, as medium movement developments, responsible for electromagnetic waves propagation. Such medium was called as the ether [11] at the times of Maxwell, Michelson and earlier. The conclusion was made in the works [1-3], that the measurement results within millimeter radio waves band can be considered as the experimental hypothesis confirmation of the material medium existence in nature such as the ether. Further discussions of the experiment results [1-3] have shown the expediency of additional experimental analysis of the ether drift problem in an optical wave band.

Experiments [7-9] and [10] are performed with optical interferometers manufactured according to the cruciform Michelson's schema [12,13]. The work of such interferometer based on the light passing in a forward direction and returning it to the observing point along the same path. The Michelson's interferometer sensitivity was low to the original ether drift effects. The measured value  $D$  in such a device, i.e. visually observed bands offset of an interference pattern expressed in terms of a visible bandwidth, is proportional to velocity ratio quadrature of the ether drift  $W$  to the light velocity  $c$ , the optical length of the light beam  $l$  and is inversely proportional to the wave length of electromagnetic emission (light)  $\lambda$  [12].

$$D = (l/\lambda) (W/c)^2. \quad (1)$$

We shall call the interval, which a beam passes in the interferometer measuring part, as the optical length of the light beam. The research methods and experiments in the investigations of the ether drift, in which the measured value is proportional  $(W/c)^2$  was called as the "methods and experiments of the second order". Accordingly the methods and experiments, in which the measured value is proportional to the first ratio extent  $W/c$  are called as the methods and experiments of the first order. The ratio is  $W/c \ll 1$  at the expected value in the experiments of Michelson, Miller  $W \approx 30$  km/sec. The methods of the second order are ineffective at this requirement. So at  $W \approx 30$  km/sec the method of the second order in 10000 (!) times succumbs on sensitivity to the method of the first order. However at that time the methods of the first order, suitable for the ether drift velocity measuring, were not known.

The expression (1) allows to estimate the difficulties, with which the explorers of the ether drift confronted

in the first attempts while observing the effects of the second order. So in the widely known first experiment of Michelson 1881 [12], at the suspected velocity value of the ether drift  $W \approx 30$  km/sec, with the interferometer having parameters:  $\lambda \approx 6 \cdot 10^{-7}$  m;  $l \approx 2.4$  m, it was expected to observe the value  $D \approx 0.04$  of the band. And it is in the requirements of considerable band shivering of an interference pattern. In the work [12] Michelson marked: *"The band were very indistinct and they were difficult for measuring in customary conditions, the device was so sensitive, that even the steps on the sidewalk in a hundred meters from the observatory caused the complete bands vanishing!"*. Later, in 1887, Michelson, also in his world-known work [14], together with E.V.Morly, once again marked the essential deficiencies of his first experiment as for the ether drift [12]: *"In the first experiment one of the basic considered difficulties consisted in the apparatus rotating without the distorting depositing, the second — in its exclusive sensitivity to vibrations. The last was so great, that it was impossible to see interference bands, except short intervals at the business-time in the city, even at 2 a.m. At last, as it was marked earlier, the value, which should be measured, i.e. the interference bands offset because of something on the interval, smaller, than 1/20 of the interval between them, is too small, to determine it, moreover at laying inaccuracies of the experiment"*.

In Miller's interferometer, for sensitivity increase, the optical path length in each of shoulders reached up to 64 meters [7-9]. It was gained due to applying of multiple reflection. The actual length of shoulders was reduced up to 4 meters. In the experiment [10] the optical length of the path reached 26 meters. In the experiments [7-9] and [10] the interferometers laid on rafts, placed in tanks with quicksilver, that allowed to remove the influence of exterior mechanical clutters.

The positive results of Miller's experiment by virtue of their general physical significance attracted the physicists' great attention at that time. In the monographs [15] 150, devoted to the ether drift's problem and referring to 1921-1930, are mentioned that almost everyone were concentrated on the discussion of Miller's results. The possible influencing of the difficult considered exterior reasons (temperature, pressure, solar radiation, air streams etc.) on the optical cruciform interferometer, sensitive to them, which had considerable overall dimensions [16] in Miller's experiments was discussed most widely in these works. Besides by virtue of methodical limitations being in the works [7-9] and [10], their authors did not manage to show experimentally correctly, that the movement, detected in their experiments, can be explained by the Earth relative movement and the medium of material origin, responsible for electromagnetic waves propagation [1-3]. However the most essential reason, which made Miller's contemporaries consider his experiments erratic, was that in numerous consequent works, for example, such as

[17-20], Miller's results were not confirmed. In the experiments [17-20] so-called the "zero results" were obtained, i.e. the ether drift was not detected.

Thus, taking into consideration the works deficiencies [7-9], [10] and a major number of experiments with a zero result available, it is possible to understand the physicists' mistrust to the works [7-9], [10] at that time, the results of which pointed the necessity of the fundamental physical concept variations. The analytical review of the most significant experiments, performed with the purpose of the ether drift search, is explained in the works [1-3, 21].

In 1933 D.K. Miller, in his summary work [22], performed the comparative analysis of multiple unsuccessful attempts of his followers to detect the ether drift experimentally. He paid attention that in all such attempts, except the experiment [10], optical interferometers were placed in hermetic metallic chambers. The authors of these experiments tried to guard the devices from exposures with such chambers. In the experiment [10] it was placed into a fundamental building of the optical workshop at the Mount Wilson observatory for stabilizing the interferometer temperature schedule. The hermetic metallic chamber was not applied, and the ether drift was detected. Its velocity had the value  $W \approx 6000$  m/sec. Miller made the conclusion: "*Massive non-transparent shields available are undesirable while exploring the problem of ether capturing. The experiment should be made in such a way that there were no shields between free ether and light way in the interferometer*".

Later, new opportunities for conducting experiments on the ether drift discovery have appeared also after the instruments occurrence based on completely diverse ideas (resonators, masers, Messbauer's effect etc.). Such experiments were held [23-26]. And again the massive metallic chamber usage was the common instrumental error of these experiments. In the works [23,24,26] there were the metallic resonators, in the work [25] — a lead chamber, because it was necessary to use gamma radiation. The authors of these works, perhaps, didn't pay attention to Miller's conclusions of 1933 about the bulk shields inapplicability in the ether drift experiments. The phenomena physical interpretation of the essential ether drift velocity reduction at metallic shields available was given by V.A. Atsukovsky for the first time, having explained major ether-dynamical metal resistance of a Fermi's surface available in them [6].

The purpose of the work is the experimental hypothesis test of the ether existence in nature within an optical electromagnetic waves band — material medium, responsible for electromagnetic waves propagation. It is necessary to solve the following problems for reaching this purpose. To take into account the deficiencies that occurred in the experiments earlier conducted. To elaborate and apply an optical measuring method and

the metering device, which does not iterate the Michelson's schema, but being its analog in the sense of result interpretation. (Michelson's interferometer of the second order is a bit sensitive to the ether streams and too sensitive to exposures.) To execute systematic measurements in the epoch of the year corresponding to the epoch of the experiments implementation [1-3], [7-9], [10]. (The term "epoch" is borrowed from astronomy, in which the observation of different years performed in the months of the same name, refer to the observations of one epoch.) The results of systematic measurements should be compared to the results of the previous experiments. The positive result of the experiment can be considered as experimental hypothesis confirmation of the ether existence in nature as material medium.

**Measuring method.** The ether model, proposed in the works [4-6], was accepted at making the experiment. The following effects should be observed experimentally within the original hypothesis:

*The anisotropy effect* — the velocity of electromagnetic waves propagation depends on radiation direction, that is stipulated by the relative movement of the solar System and the ether - the medium, responsible for electromagnetic waves propagation.

*The height effect* — the velocity of wave propagation depends on the height above the Earth's surface, that is stipulated by the Earth's surface interaction with the viscous ether stream - material medium, responsible for electromagnetic waves propagation.

*The space effect* — the velocity of wave propagation changes its value with a period per one stellar day, that is stipulated by a space (galactic) origin of the ether drift — the medium, responsible for electromagnetic waves propagation. Thus the height (astronomical coordinate) of the Solar system movement apex will change its value with the period per one stellar day as well as for any star owing to the Earth's daily rotating. Therefore the velocity horizontal component of the ether drift and, hence, the velocity of electromagnetic wave propagation along the Earth's surface will change the values with the same period.

*The hydroaerodynamic effect* — the velocity of electromagnetic waves propagation depends on movement parameters of viscous gas-like ether in directing systems (for example, in tubes), that is stipulated by solids interaction with the ether stream — material medium, responsible for electromagnetic waves propagation. (As it is known, the law of fluids and gases motions and their interaction with solids is learnt by hydroaerodynamics. This effect, apparently, should be called as the *ether-dynamics* effect with reference to the ether dynamics. It can be seen, that "the height effect" is referred to the etherdynamic effect class. However in the work, by virtue of methodical reception distinction used for their discovery, the effects are indicated as separate).

According to the investigation purpose, the measuring method should be sensitive to these effects.

The following model statements are used at measuring method development [4-6]: the ether is a material medium, responsible for electromagnetic waves propagation; the ether has properties of viscous gas; the metals have major etherdynamic resistance. The imagination of the hydroaerodynamic (etherdynamic) effect existence is accepted as the initial position. The method of the first order based on known regularities of viscous gas movement in tubes [27-28] has been proposed and realized within the optical electromagnetic waves band in the work for measuring of the ether drift velocity and ether kinematic viscosity.

The method essence is in the following. Let's place a tube part into a gas stream in such a way, that the direct tube axis will be perpendicular to the stream velocity vector. In this case both opened tube ends in relation to an exterior gas stream are in identical conditions. The gas pressure drop does not occur on the tube part, and the gas inside a tube will be immobile. Then we shall turn a tube in such a way, that the velocity vector of a gas stream will be directed along the tube axis. In this case the gas speedy stream will create a pressure drop on the tube ends, under action of which there is a gas stream in a tube soon. The stabilization time of a gas stream in a tube and this stream velocity are determined by the values of gas kinematic viscosity, the geometrical tube sizes and the velocity of an exterior gas stream [27-28]. Let's mark, that the development of constant gas stream in a tube lasts a terminating interval of time. The ether is a gas-like material medium, responsible for electromagnetic waves propagation according to the accepted hypothesis. It means, that the electromagnetic wave velocity regarding to the observer is the sum of wave velocity vectors relative to the ether and the ether velocity with regard to the observer. In this case, if an optical interferometer is created, in which a beam drives inside a metallic tube, and another outside of a tube (in the ether exterior stream) and to turn the interferometer in the ether drift stream, it can be expected, that in such interferometer, during a stabilization time of the ether stream in a tube, the bands offset of the interference pattern regarding to the original position of these bands on the interferometer scale should be observed. Thus the value of bands offset will be proportional to the ether exterior stream velocity, and the stabilization time — the bands return time to the original position, will be defined by the ether kinematic viscosity value. Hence, the proposed measuring method enables to meter the ether drift velocity values and the ether kinematic viscosity. The proposed measuring method is a method of the first order, as it is not required to revert a light beam to the initial point (as, for example, in Michelson's interferometer).

Let's calculate the interferometer parameters. For the stream analysis of the gas-like ether we shall use the mathematical hydrodynamics apparatus, which is advanced in the works [27-28] at the problem solving,

connected with the stream of viscous incompressible fluid. The use of such solutions for gas stream analysis is true, if the following requirement is performed

$$0.5Ma^2 \ll 1, \quad (2)$$

where  $Ma = w_{pa}c_s^{-1}$  is a Mach's number;  $w_{pa}$  is an average gas stream velocity on a tube section;  $c_s$  is the gas sound velocity. At the requirement implementation (2), it is possible to neglect the gas pressure effects and consider the gas stream as the stream of incompressible fluid. On data of the experimental works [1-3], [7-9] and [10], the ether drift velocity  $W$  near the Earth's surface does not exceed the value  $W \approx 10^4$  m/sec. In the work [6] the sound velocity in the ether is estimated by the value  $c_s \approx 10^{21}$  m/sec, that essentially exceeds the light velocity. Even if to consider, that  $c_s = c$ , we shall receive, that  $Ma \approx 3.3 \cdot 10^{-5}$ . Hence, the requirement (2) is performed, the stream of a gas-like ether can be considered as a stream of viscous incompressible fluid and the use of the hydrodynamics corresponding mathematical apparatus is true for ether stream analysis.

Laminar and turbulent fluid streams are distinguished in hydrodynamics. The laminar fluid stream exists, if the Reynolds number  $Re$ , drawn up for a stream, does not exceed some extreme value  $Re_c$  [27-28]

$$Re < Re_c. \quad (3)$$

The Reynolds number for a round cylindrical tube is defined by the following expression

$$Re = 2a_p w_{pa} \nu^{-1}, \quad (4)$$

where  $a_p$  is the interior tube radius;  $\nu = \mu\rho^{-1}$  is kinematic fluid viscosity;  $\mu$  is the dynamic viscosity;  $\rho$  is the fluid density. Depending on the exterior stream nature and the requirements of fluid influx into a tube, the values  $Re_c$  are within  $Re_c \approx 2.3 \cdot 10^3 \dots 10^4$ . At  $Re < 2.3 \cdot 10^3$  the fluid stream in a tube exists only as laminar and does not depend on an extent of an exterior stream turbulence. The following features are peculiar for a steady laminar fluid stream in a round cylindrical tube. The particle movement pathways are rectilinear. The maximal fluid stream velocity  $w_{pmax}$  takes place along the tube axis and is equal to

$$w_{pmax} = 0.25\Delta p a_p^2 \mu^{-1} l_p^{-1}, \quad (5)$$

where  $\Delta p$  is the pressure drop on a tube part with the length  $l_p$ ;

$$\Delta p = 0,25\gamma_p l_p a_p^{-1} \rho w_{pa}^2; \quad (6)$$

$\gamma_p$  is the coefficient of a round tube resistance, which is equal  $\gamma_p = 64Re^{-1}$  at a laminar regime of fluid stream. The maximal stream velocity  $w_{pmax}$  is twice more than mean fluid velocity

$$w_{pmax} = 2w_{pa}. \quad (7)$$

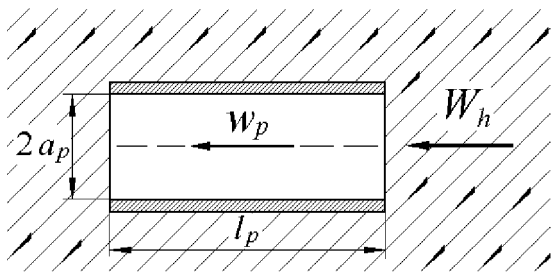


Figure 1: A tube in a gas stream

The stream velocity distribution on a tube section is called as Puazeyl's parabola and looks like

$$w_p(r) = w_{pmax} (1 - r^2 a_p^{-2}), \quad (8)$$

where  $r$  is the coordinate along the tube radius.

The laminar stream transferring into a turbulent one takes place not fluently, but by jumps. At transferring through the extreme value of a Reynold's number the tube resistance coefficient increases by jump, and then slowly reduces. The following features are peculiar for a steady stream of viscous liquid in a round cylindrical tube of turbulent stream. The pathways of particle movement have scattered nature. The resistance coefficient of a round tube is equal  $\gamma_p = 0.3164 Re^{-0.25}$ . The velocity distribution on a tube section is almost uniform with their sharp reduction up to zero point in a thin layer near the wall. The maximal velocity increase above the mean order value is about 10-20 % [27-28]

$$w_{pmax} \approx (1.1 \dots 1.2) w_{pa}. \quad (9)$$

It will be shown below, that in the experiment requirements, as a rule,  $Re > Re_c$ , therefore in the work we shall be restricted by the estimations, performed for the ether turbulent stream.

Let's consider the method operating principle. In the Fig. 1 the part of a cylindrical round metallic tube with the length  $l_p$ , which is in the ether stream (ether drift), is shown

The ether stream is shown in the figure as slanting thin lines with arrows, that indicate the direction of its movement. The tube longitudinal axis is located horizontally and along with the ether drift velocity vector is in a vertical plain, which represents the figure plain. The tube walls have major ether-dynamic resistance and the ether stream acting from the tube surface side area, the ether inside a tube does not move. The ether velocity stream stipulated by the horizontal velocity component of the ether drift  $W_h$ , creates the ether stream in a tube, which goes with the mean velocity  $w_{pa}$ . It can be spoken, that the metallic tube is the routing system for the ether stream. Let's turn a tube in a horizontal plain in such a way, that its longitudinal axis will take up a position perpendicular to

the plain of the Fig. 1 or, that is similar — perpendicular to the velocity vector of the ether drift. In this position both opened ends of a tube will be in identical conditions regarding to the ether stream, the pressure differential  $\Delta p$  does not occur and according to (5) the ether stream velocity in a tube is equal to a zero point. At the moment  $t_0$  we shall turn a tube into the initial position. The horizontal component of the ether drift velocity  $W_h$  will create a pressure drop  $\Delta p$  on the tube ends, under operation of which the ether stream will be developed in a tube. In the work [28] the problem about setting into motion of viscous incompressible fluid being in a round cylindrical tube under operating of the suddenly appended constant pressure drop  $\Delta p$  is solved. Let's reduce the formula of the velocity distribution of fluid stream in a tube

$$w_p(r, t) = w_{pmax} \left[ 1 - \frac{r^2}{a_p^2} - 8 \sum_{k=1}^{\infty} \frac{J_0(\psi_k r a_p^{-1})}{\psi_k^3 J_1(\psi_k)} \exp\left(-\frac{\nu \psi_k^2 t}{a_p^2}\right) \right], \quad (10)$$

where  $t$  is the time;  $\psi_k$  is the equation roots  $J_0(\psi_k) = 0$ ;  $J_0$ ,  $J_1$  are Bessel's functions of the zero and first orders. The first two summands in square brackets express steady (at  $t \rightarrow \infty$ ) laminar stream of fluid and correspond the mentioned above "Puazeyl's parabola" (8). So at a turbulent fluid stream, according to (9), the velocity distribution on a tube section is almost uniform, we shall consider, that the fluid stream velocity is equal  $w_{pa}$  on the whole tube section (the value  $\gamma_p$  of the round tube at a turbulent fluid stream should be used at the value calculation  $w_{pa}$ ) except the thin near-wall layer. In this case the expression (10) at  $r = 0$  will be like

$$w_p(t) \approx w_{pa} \left[ 1 - 8 \sum_{k=1}^{\infty} \psi_k^{-3} J_1^{-1}(\psi_k) \cdot \exp(-\nu \psi_k^2 a_p^{-2} t) \right]. \quad (11)$$

The expression (11) describes the process of a fluid stream defining in a round tube. It follows from (11), that at  $t \rightarrow \infty$  the value is  $w_p(t) \rightarrow w_{pa}$ . Both parts of the expression (11) should be divided into the value of constant fluid stream velocity in a round tube  $w_{pa}$ . In this case the time variation of fluid stream dimensionless velocity  $w_p(t)/w_{pa}$  will be like, that is shown in a Fig. 2.

In the figure the values of dimensionless velocity  $w_p(t)/w_{pa}$  are given on an ordinates axis, the values of time are given on the abscissa axis. As it is shown above, the requirement (2) is performed and the ether stream can be described by the laws of thick liquid motions, then we shall speak about the ether stream further, instead of fluid. In the Fig. 2 we'll allocate the

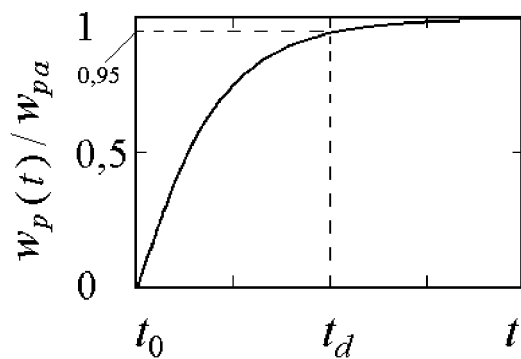


Figure 2: Variation in time of fluid movement velocity in a tube

interval of time  $t_0 \dots t_d$ , during which the ether stream velocity in a tube changes from 0 up to  $0.95 w_{pa}$ . We shall call the ether stream regime on this time interval as the dynamic one. We shall call the ether stream regime at  $t > t_d$  as the steady stream regime.

Let's skip a light beam along the tube axis. It can be written down, that the phase of a light wave on a cut with the length  $l_p$  will vary on value  $j$ , which is equal.

$$\varphi = 2\pi f l_p V^{-1}, \quad (12)$$

where  $f$  is the electromagnetic wave frequency;  $V$  is the light velocity in a tube. According to the original hypothesis the ether is a medium, responsible for electromagnetic waves propagation. This implies, that if in a tube with the length  $l_p$  there is the ether stream, the velocity of which changes in time, so the phase of a light wave measured on the tube output, should change in time according to variation in time of the ether stream velocity  $w_p(t)$ . Then the expression (12) will be like

$$\varphi(t) = 2\pi f l_p [c \pm w_p(t)]^{-1}, \quad (13)$$

where  $c$  is the light velocity in a fixed ether, in vacuum. In the expression (13) the sign "+" is used, when the direction of the light propagation coincides with the ether stream direction in a tube, and the sign "-" is used, when these directions are opposite.

In the work the optical interferometer is applied for measuring value  $\varphi(t)$ . Rozhdestvensky's interferometer schema is taken [29] as the basis, which is supplemented in such a way, that the light beam drove along the empty metallic tube axis in one of the shoulders. The interferometer schema and its basic clusters are shown in the Fig. 3.

1 — illuminator; 2 — a metallic tube part; 3 — eyefragment with a scale;  $P_1, P_2$  — flat parallel semi-transparent laminas;  $M_1, M_2$  — mirrors are shown on the schema. The beam course is shown with thick lines and arrows. The light beam in a tube pass along the axis and is indicated with a broken line in the figure. The tube length is  $l_p \approx P_1M_1$ . The clusters  $P_1, M_1$

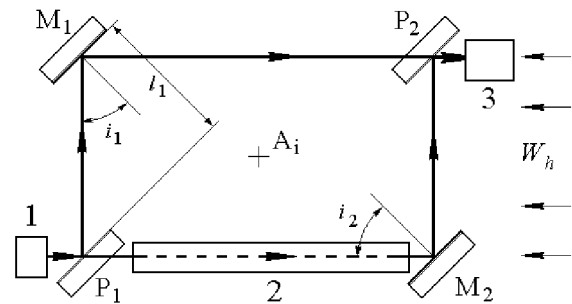


Figure 3: The schema of an optical interferometer

and  $P_2, M_2$  are mounted two by two parallelly,  $M_1, M_2$  are mounted opposite each other on a small angle. The angles  $i_1, i_2$  are the angles between normals to the mirror plains  $M_1, M_2$  and the beams dropping on them. The intervals are  $P_1M_1 = M_2P_2 = l_1, M_1P_2 = P_1M_2 \approx l_p$ . In a classical case if the ether drift influence isn't considered, the Rozhdestvensky's interferometer operating is reduced to the following. The light beam with the wave length  $\lambda$  is divided  $P_1$  into two beams, which after reflection from  $M_1$  and  $M_2$  and passing  $P_2$  are parallel with a phase difference [29]

$$\delta = 4\pi l_1 \lambda^{-1} (\cos i_1 - \cos i_2). \quad (14)$$

The angles  $i_1, i_2$  are established at the interferometer adjustment so that the interference pattern should be observed. (The adjustment clusters are not shown on the schema symbolically). In a tuned interferometer the value is  $\delta = const$ . In the right part of the Fig. 3 the family of arrows means the stream direction of the ether drift horizontal component velocity. This stream velocity is equal to  $W_h$ . If to arrange the interferometer clusters on a horizontal rotated background, such instrument can be turned in the ether stream. The rotation axis is perpendicular to the figure plains and is indicated as  $A_i$ .

In the interferometer (Fig. 3) the band position of an interference pattern regarding to the eyefragment scale 3 is defined by the phase difference of the light beams, which are distributed on the paths  $P_1M_2P_2$  and  $P_1M_1P_2$ . In the Fig. 3 the ether stream is directed towards the light propagation direction along the beams  $P_1M_2, M_1P_2$ . In this case, according to (13), we shall write down expression for the phase difference  $\Delta\varphi(t)$  between the beams  $P_1M_2P_2$  and  $P_1M_1P_2$ .

$$\Delta\varphi(t) = 2\pi f \left\{ \left[ \frac{P_1M_2}{c - w_p(t)} + \frac{M_2P_2}{c} \right] - \left( \frac{P_1M_1}{c} + \frac{M_1P_2}{c - W_h} \right) \right\} + \delta, \quad (15)$$

where  $\delta$  is constant, the value of which is defined by the expression (14). Let's simplify the expression (15).

For this purpose we shall introduce the identifications accepted earlier. Allowing, that the beam phase difference  $M_2P_2$  and  $P_1M_1$  does not depend on the interferometer orientation regarding to the ether stream direction and is equal to zero point, the expression for the value  $\Delta\varphi(t)$  will be like

$$\Delta\varphi(t) = 2\pi fl_p \left[ \frac{1}{c - w_p(t)} - \frac{1}{c - W_h} \right] + \delta. \quad (16)$$

The first member of the expression (16) describes the beam phase variation  $P_1M_2$  depending on the ether stream velocity in a tube  $w_p(t)$ . The second member is the beam phase variation  $M_1P_2$  depending on the ether exterior stream velocity  $W_h$ . Let's reduce the expression in square brackets to a communal denominator and, allowing, that  $c^2 \gg W_h w_p(t) - c w_p(t) - c W_h$ ,  $fc^{-1} = \lambda^{-1}$  we shall receive

$$\Delta\varphi(t) \approx \frac{2\pi l_p}{\lambda} \left[ \frac{w_p(t) - W_h}{c} \right] + \delta. \quad (17)$$

It follows from the expression (17), that the difference in the phase  $\Delta\varphi(t)$  between beams  $P_1M_2P_2$  and  $P_1M_1P_2$  is proportional to a differential of the ether stream velocity in a tube  $w_p(t)$  and the ether exterior stream  $W_h$ .

Let's consider the interferometer operating in its steady regime, at  $t \rightarrow \infty$ . According to the expression (11) and Fig. 2  $w_p(t)_{t \rightarrow \infty} \rightarrow w_{pa}$  it can be suspected, that owing to the small value of the ether dynamic viscosity (celestial bodies move in the ether) the ether steady stream velocity in a tube regarding to the small length will not differ essentially from the ether exterior stream velocity and it is possible to write down, that  $w_p(t)_{t \rightarrow \infty} = w_{pa} \approx W_h$ . (The correctness of this supposition in the work is determined experimentally and shown below.) In this case in the expression (17) the fraction numerator in square brackets is equal to zero point, and this expression will be

$$\Delta\varphi(t)_{t \rightarrow \infty} \approx \delta. \quad (18)$$

Hence, in the steady regime the interferometer operating with a metallic tube does not differ from the Rozhdestvensky's interferometer operating. In both interferometers the bands position of an interference pattern will be defined by the original phase difference  $\delta$ . The interferometer, with a metallic tube, in the steady operating regime is not sensitive to the ether drift velocity and can not detect the availability or absence of the ether drift.

Let's consider a dynamic operating regime of the interferometer. Let's unroll the interferometer (see Fig. 3) in the horizontal plain at  $180^\circ$ . As the direction of the light propagation has varied in relation to the ether drift stream to the opposite one, the expression (17) will be like

$$\Delta\varphi(t) \approx \frac{2\pi l_p}{\lambda} \left[ \frac{W_h - w_p(t)}{c} \right] + \delta. \quad (19)$$

According to the expression (11) and the Fig. 2, the inequality  $w_p(t) < W_h$  takes place at the time interval  $t_0 \dots t_d$ . Hence, in a dynamic regime the interferometer with a metallic tube is sensitive to the velocity differential of the ether exterior stream velocities  $W_h$  and the ether stream inside a tube  $w_p(t)$ . We shall discover the bands offset value of the interference pattern regarding to their position in the interferometer steady work regime as follows. Let's take a differential of the expressions (19), (18) and divide both parts of the found expression into  $2\pi$ , we shall receive

$$\frac{\Delta\varphi(t) - \Delta\varphi(t)_{t \rightarrow \infty}}{2\pi} = \frac{l_p}{\lambda} \left[ \frac{W_h - w_p(t)}{c} \right]. \quad (20)$$

The expression left-hand part (20) is equal to the required interference pattern offset, which is expressed by the number of electromagnetic wave periods. With reference to the visually observed interference pattern the expression (20) describes the value variation in time of visible bands offset of this pattern regarding to their original position —  $D(t)$ . The visible bandwidth value of an interference pattern can be the offset measurement unit. Taking into consideration, that the ether stream in a tube can have the direction opposite to the selected on the Fig. 3, generally it is possible to receive

$$D(t) = \pm \frac{l_p}{\lambda} \left[ \frac{W_h - w_p(t)}{c} \right]. \quad (21)$$

In the expression (21) the sign "+" is used, when the light propagation direction coincides with the ether stream direction in the interferometer dynamic regime in a tube, and the sign "-" is used, when these directions are opposite. According to the expression (11) and the Fig. 2 at an instant  $t_0 = 0$  the ether stream velocity in a tube is  $w_p(t_0) = 0$ . Then from (21) we shall receive, that at the instant  $t_0$  the bands offset of an interference pattern accepts the maximal value equal to

$$D(t_0) = \pm \frac{l_p}{\lambda} \cdot \frac{W_h}{c}, \quad (22)$$

and in the steady regime, when the ether velocity in a tube is equal to  $w_p(t)_{t \rightarrow \infty} \approx W_h$ , the bands offset regarding to their original position is equal 0. The dependence view  $D(t)$  can be obtained with the dependence  $w_p(t)/w_{pa}$ , which is shown in the Fig. 2. Really, let's divide (21) into (22), we shall receive

$$\frac{D(t)}{D(t_0)} = 1 - \frac{w_p(t)}{W_h}. \quad (23)$$

Allowing the supposition made above, that  $w_p(t)_{t \rightarrow \infty} = w_{pa} \approx W_h$  the expression (23) can be written down as  $D(t)/D(t_0) \approx 1 - w_p(t)/w_{pa}$ . The dependence view obtained in such a way, is shown in the Fig. 4

In the expression (22) the measured value  $D$  is proportional to the first extent of the ether drift velocity ratio to the light velocity, that characterizes the reviewed

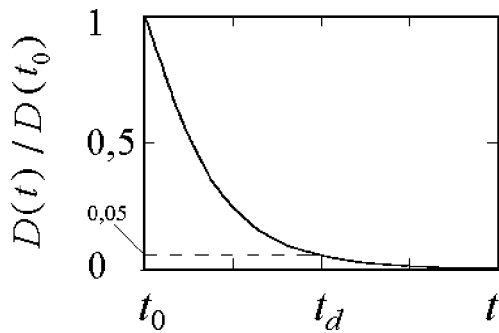


Figure 4: Variation in time of interference pattern bands offset in a dynamic interferometer operating regime

method as the first order method. It follows from the expression (22) and the Fig. 4, that if at the moment of time  $t_0$  to measure the bands offset value  $D$  regarding to their original position on the interferometer eyefragment scale, it is possible to determine the ether drift velocity horizontal component  $W_h$  which is equal to

$$W_h = \pm D(t_0) c \lambda t_p^{-1}, \quad (24)$$

The direction of the interference pattern bands offset, regarding to their original position, will be defined by the ether exterior stream direction.

The data of the interferometer tube sizes are necessary for the proposed measuring method realization. The expression for the tube interior radius calculation  $a_p$  can be obtained as follows. Let's divide both parts of the expression (11) on  $w_{pa}$  and, allowing, that at the moment of time  $t_d$  (see the Fig. 2) the ratio  $w_p(t)/w_{pa} = 0.95$ , we shall write down as

$$1 - 8 \sum_{k=1}^{\infty} \psi_k^{-3} J_1^{-1}(\psi_k) \exp(-\nu \psi_k^2 a_p^{-2} t_d) = 0.95. \quad (25)$$

If to be confined by the estimation accuracy no worse than 7 %, so the series in the expression (25) can be exchanged by its first member. Let's substitute in the (25) the numerical values  $\psi_k$  and  $J_1(\psi_k)$  (for the information we shall give these values:  $\psi_1 = 2.4048$ ;  $J_1(\psi_1) = 0.5191$ ), we shall receive

$$a_p \approx 1.37 (t_d \nu)^{1/2}. \quad (26)$$

The expression (26) allows to calculate such the interferometer design parameter as the tube radius  $a_p$ . At calculation, the value  $t_d$  is selected coming from the time, which is required for implementation of visual (or tool) readout of bands offset value  $D$ . The data of the ether kinematic viscosity value  $\nu$  will be reviewed

below. The tube length  $l_p$  can be found with the expression (24), of which we shall receive

$$l_p \approx D_{min}(t_0) \lambda c W_{hmin}^{-1}, \quad (27)$$

where  $D_{min}(t_0)$  is bands offset minimum value of an interference pattern, which can be digitized with the selected eyefragment and scale;  $W_{hmin}$  is the minimum value of the ether drift horizontal component velocity, which should be measured by the interferometer (the interferometer sensitiveness).

**The ether kinematic viscosity.** The data of the ether kinematic viscosity value  $\nu$  are necessary for the measuring method realization. Let's estimate the value  $\nu$ , relying on the following. In the work [5] the photon formation mechanism is represented, as the oscillating result of excited atom electronic shell in the ether and the Karman's vortex track as hydromechanical photon model is proposed. In other words the photon formation is stipulated by the ether stream turbulent regime of the excited atom streamlining by the ether, oscillating in the ether. The turbulent pulsation propagation in the ether is perceived by the observer as the light emission. In the work [28] it is shown, that the existence of pulsation movement is possible in fluid volume, if the Reynold's number is not lower than some extreme value equal to

$$Re_{cr} = w d \nu^{-1}, \quad (28)$$

where  $w$  is fluid movement velocity;  $d$  is the characteristic size of a streamlined body. In the work [28] it is obtained, that  $Re_{cr} \approx 425$ . With reference to our problem the values  $w$ ,  $d$ ,  $\nu$  are accordingly: the ether movement velocity, atom diameter, the ether kinematic viscosity. From the expression (28) we shall find

$$\nu \approx w d Re_{cr}^{-1}. \quad (29)$$

We shall call the obtained ether kinematic viscosity value as the calculated ether kinematic viscosity value  $\nu_c$ . Let's calculate the value  $\nu_c$ . As the ether stream velocity  $w$  we shall accept the offset velocity of electronic atom shells in the immobile ether at a photon emission. Let's consider, that this velocity does not exceed the light velocity  $w \leq c$ . The diameter of atoms, as it is known, has the value order  $d \approx 10^{-10}$  m. In this case with the (29) we shall receive

$$\nu_c \leq 7.06 \cdot 10^{-5} \text{ m}^2 \text{sec}^{-1}. \quad (30)$$

The performed estimation has shown, that the ether kinematic viscosity calculated value corresponds to the work imaginations [6] about the ether as gas-like medium with real gas properties. So, the kinematic viscosity values of twelve gases, spread in nature, are within  $7 \cdot 10^{-6} \text{ m}^2 \text{sec}^{-1}$  (carbon dioxide) up to  $1.06 \cdot 10^{-4} \text{ m}^2 \text{sec}^{-1}$  (helium).



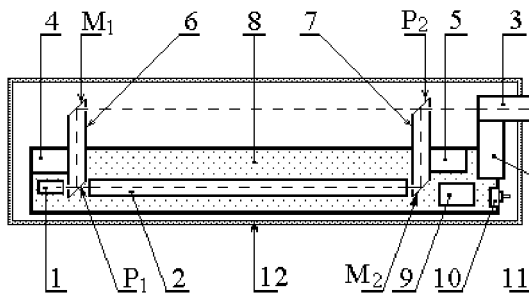


Figure 5: The interferometer structure

**Optical interferometer.** The calculated ether kinematic viscosity value allows to calculate the interferometer parameters. With the expression (26) we shall determine the tube radius. If the value  $t_d$  is supposed to be equal 1 second, we shall receive, that at the interferometer creation it is necessary to apply the tube with the interior radius  $a_p \approx 0.05$  m. We shall determine the tube length  $l_p$  with the expression (27). If to suppose the values  $D_{min} = 0.05$ ,  $W_{hmin} = 20$  m/sec and apply the light source with the wave length  $\lambda = 6.5 \cdot 10^{-7}$  m, so the required tube length is equal to  $l_p \approx 0.49$  m.

The optical interferometer was manufactured for conducting measurements. Schematic figure of the device (the top view) is shown in the Fig. 5.

In the Fig. 5 the identifications of the basic clusters are kept, which were introduced at viewing the interferometer schema (Fig. 3). 4,5 — the interferometer adjustment clusters; 6,7 — racks for fixing flat-parallel semi-transmitting laminas and mirrors; 8 — interferometer frame; 9 — power supply accumulators of the illuminator; 10 — the illuminator switch; 11 — the eyefragment fixing cluster; 12 — heat-insulating housing are shown additionally. The frame 8 is manufactured of a steel profile with II — like section. The wall thickness is 0.007 m. The profile height is 0.02 m. The frame length is 0.7 m, the width is 0.1 m. The interferometer clusters are fixed on a flat frame surface. The racks 6, 7 are manufactured of rectangular copper tubes with interior section  $0.01 \text{ m} \times 0.023 \text{ m}$ . The light beams pass inside these tubes. The interval between beams is  $P_1M_2$  and  $M_1P_2$  it is equal 0.12 m. On racks, in the points  $P_1$ ,  $P_2$  the flat parallel semi-transmitting laminas, in the points  $M_1$ ,  $M_2$  — mirrors are installed. (In the manufactured interferometer the flat parallel glasses with the thickness 0.007 m were used as semi-transparent laminas). The laminas, mirrors and clusters of their fixing in the Fig. 5 are not shown symbolically. Each of the clusters 4,5 allows to change the racks position in two orthogonal related plains. The tube 2 is steel with the interior radius  $a_p = 0.0105$  m. The

tube length is  $l_p = 0.48$  m. The clusters of the tube fixing on 5 are not shown symbolically. The semiconductor laser with the wave length  $\lambda \approx 6.5 \cdot 10^{-7}$  m was applied as the illuminator. The optical paths in the interferometer are located in a horizontal plain. The interferometer was located on a rotated material table, which was manufactured of an organic glass with the thickness 0.02 m. The heat-insulating gasket was put between the frame and material table. The interferometer was closed by a common housing of six layers of a soft heat-insulating material. The thickness of such coating was about 0.025 m. In the Fig. 5 the housing perimeter is shown. The housing background was the box of rectangular section with the interior sizes: width  $b_c = 0.22$  m, height  $h_c = 0.11$  m, length  $l_c = 0.8$  m. The box was manufactured of a cardboard with the thickness 0.007 m. In the box the face wall on the eyefragment part was absent. This opening was closed with a common soft housing. The interferometer rotating was ensured with the end thrust bearing of the diameter 0.075 m. The bearing box is located between the material table and support. The support is provided with the units for the interferometer installation in a horizontal position.

**The interferometer test.** In the manufactured interferometer the minimum bands offset of an interference pattern, which could be visually digitized, meant  $D_{min} = 0.05$ .

The device stiffness was tested by two methods. According to the first method the instrument frame was mounted on a horizontal surface. The interferometer for one edge of a frame was hoisted in such a way, that the frame lean angles to the surface plain reached  $\approx 20^\circ$ . In this position the interference patterns offset frame, stipulated by elastic deformations of the instrument, did not exceed 0.3 bands ( $D = 0.3$ ). According to the second method the instrument stiffness was tested in a working position. The frame lean angles up to  $10^\circ$  were created by the material table tilt. In this case the bands noticeable drift was not observed. The stability of an interference pattern to impulsive loads was tested. The light shocks on the interferometer frame, material table and support caused short-lived interference pattern wince at the moments of such strikes. Thus the interference pattern was not destroyed. The bands saved an original position after termination of impulsive loads.

The second stage of tests was performed on the terrain selected for experimental investigations. In windy weather the interference pattern was stable. The observer moving in an immediate proximity from the interferometer installation site, the movement of the pedestrians and cars in 20 meters from the instrument installation site did not cause the noticeable offset or bands shivering. The short-lived bands shivering at cars movement was marked on one of two selected points, which was in seven meters from a ground road. Thus the interference pattern was observed, and the bands

did not change the position. (The transport movement in this terrain is insignificant — on the average 3-4 automobiles per a day.)

The interferometer heat tests were held in summer. The device was mounted on the open site. The various device orientation on an azimuth was set in cloudless weather conditions. In a fixed position the instrument was heated by solar radiation. In these conditions within 30 minutes the bands offset did not exceed the value  $D = 0.35$  ( $\approx 1/100$  bands for a minute). In cloudy weather and at night the interference pattern saved an invariable position within 2-3 hours.

The measuring method sensitiveness to the ether drift required effects was tested at the test final stage. The method of interferometer application was the following. The instrument was mounted in a horizontal position in such a way, that its direct axis coincided with a meridian line, and the illuminator was turned to the north. In such initial position, in the interferometer steady work, the observer registered the bands original position of an interference pattern regarding to the eyefragment scale. The value  $D = 0$  was given to the bands original position. Then the observer changed the position — took a seat at the illuminator. The interferometer turned in  $180^\circ$ . The rotational displacement was performed within three seconds. At rotational displacement, as it was reviewed above, the ether stream in a tube was interrupted. The interferometer transferred into a dynamic operating regime, which is described by the expression (11). In this interferometer position the maximal value of bands offset, the bands release time to their original position was registered. The interferometer transferred into a steady regime, and turned into the initial position. At this stage of tests it was established, that after the dynamic regime termination the bands noticeable offset of an interference pattern regarding to their original position was not observed, i.e. bands offset value  $D(t)_{t \rightarrow \infty} \approx 0$ . According to the expression (21) it means, that the ether stream velocity along the tube axis at  $t \rightarrow \infty$  differed a bit from the ether exterior stream velocity, that the value  $D$  was behind the interferometer threshold. It can be explained by small resistance of the interferometer tube to the ether stream movement inside this tube. Let's consider in this case, that

$$w_p(t)_{t \rightarrow \infty} = w_{pa} \approx W_h. \quad (31)$$

This experimental result was used above at the proportion deduction (18).

At procedure implementation, described above, it was marked, that at the whole time course of value  $D$  variations corresponded to variations, which are shown in the Fig. 4 that did not contradict the original imaginations about the interferometer work. The measured duration of a dynamic regime meant  $t_d \approx 10 \dots 13 \text{ sec}$ . The values ambiguity  $t_d$  is stipulated, first of all, by the

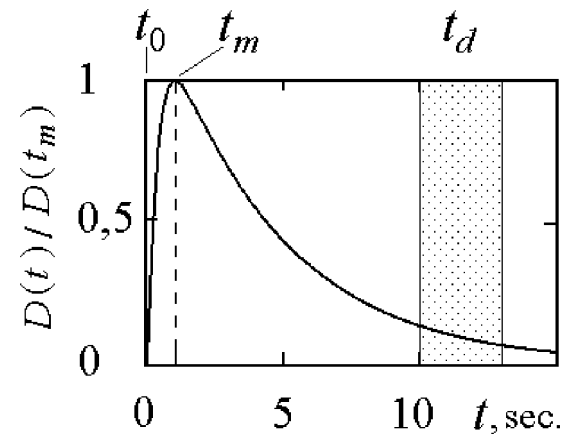


Figure 6: Observed variation in time of the interference pattern bands offset in the interferometer dynamic operating regime

difficulties, connected with small values visual readout of the value  $D$ , slowly changing, at the dynamic regime end, i.e. at  $t \rightarrow t_d$ . In the Fig. 6 the dependence view  $D(t)$ , created on the data visual observations, is shown.

However, as it can be seen in the Fig. 6, on the original site by the extent about 1 second the dependence time course  $D(t)$  differed from an expected time course qualitatively. After the device rotation in  $180^\circ$ , at the moment of time  $t_0$ , the bands still occupied the initial position, i.e.  $D(t_0) = 0$  instead of anticipated, according to (22) and the Fig. 4, the value  $D(t_0) = \text{max}$ . Since the moment  $t_0$ , the value  $D$  within the time  $t_m \approx 1 \text{ sec}$  reached the maximal value. There were suppositions of certain mechanical stresses influencing at the interferometer braking after its rotation in  $180^\circ$  or other reasons, connected, for example, with air movement inside a heat-insulating housing. In this connection different methods of the interferometer starting into movement and its braking were tested. The tests have shown, that the observed feature of the interferometer work could not be explained by the suppositions made. The systematic round-the-clock tests have shown the following. The daily variations of the value  $D$  corresponded the measured ones in the experiment [1-3] to the ether drift velocity variations within a day. (In the experiment [1-3] round-the-clock measurements were carried out continuously during 13 months, since August 1998 till August 1999. The part of this experiment results is published in the works [1-3]. The measurement results within radio waves band have shown, that there is a rather small value of the ether drift horizontal component velocity during the part of a day. The same effects were marked at the optical interferometer test in the work. The experience has shown, that at a separate day, on such periods of time at the interferometer rotation on  $180^\circ$  the no-

ticeable bands offset of an interference pattern was not observed. Hence, the detected features in dependence  $D(t)$  (Fig. 6) could not be caused by the interferometer mechanical strains or air movements inside the interferometer heat-insulating housing, and are stipulated by the exterior reasons. Such time periods, during which  $D(t_m) \approx 0$  were used for improvement ways of the interferometer starting in rotation and its stopping. These ways were used then as standard procedures at systematic measurement conducting.

**Analysis of the interferometer test results.**

The detected regularity in the observed bands offset has required its physical interpretation. The possible influencing analysis of the interferometer structural elements on the ether streams has shown, that the observed dependence features  $D(t)$  can be qualitatively and quantitatively described within the following supposition. Let allow, that an exterior heat-insulating dielectric housing of the interferometer (the point 12 in the Fig. 5) forms the additional directing system for the ether stream drift, besides a metallic tube. In this case the exterior in relation to a metallic tube of the ether stream is the ether movement in a dielectric housing. If to consider the interferometer housing as the routing system, it is necessary to consider, that, since the moment  $t_0$  in it, as well as in a metallic tube, the dynamic process of the ether stream defining will be developed. It gives the basis to write down the expression (21) as follows

$$D(t) = \pm \frac{l_p}{\lambda} \left[ \frac{W_c(t) - w_p(t)}{c} \right], \quad (32)$$

where  $W_c(t)$  is the variation of the ether stream velocity in time in the interferometer housing;  $w_p(t)$  is the variation of the ether stream velocity in time in a metallic tube.

The housing basis was a cardboard box of rectangular section. Let's consider a problem about setting the ether into motion, resting in a rectangular tube. For this purpose let's use the comparative method, spread in hydrodynamics, of fluid stream in a tube of a compound profile with fluid stream in the tube of round section, "equivalent" on resistance, at which so-called "hydraulic" radius  $a_h$  equal to an area ratio of a tube normal section  $G_p$  to the section perimeter  $N_p$  is accepted [27] for this radius

$$a_h = G_p N_p^{-1}. \quad (33)$$

Such a way enables to use the mathematical apparatus developed at stream analysis in round tubes. As before we shall be limited to estimations, performed for the ether turbulent stream. In this case the dependence  $W_c(t)$  can be calculated with the expression similar to the expression (11) in which as the round tube radius

$a_p$  we shall use the "hydraulic" radius of a rectangular tube  $a_h$

$$W_c(t) \approx w_{pac} \left[ 1 - 8 \sum_{k=1}^{\infty} \psi_k^{-3} J_1^{-1}(\psi_k) \cdot \exp(-\nu \psi_k^2 a_h^{-2} t) \right], \quad (34)$$

where  $w_{pac}$  is a mean velocity of the ether steady turbulent stream in the interferometer dielectric housing. As before, at considering the expression (17), and taking into account the interferometer test results (31), it is possible to consider, that the value  $w_{pac}$  does not differ essentially from the ether exterior stream velocity  $W_h$  and it is possible to write down

$$W_c(t)_{t \rightarrow \infty} = w_{pac} \approx W_h. \quad (35)$$

Let's calculate the value  $a_h$ . Above, the housing interior overall dimensions were given at the interferometer structure description: width  $b_c = 0.22$  m, height  $h_c = 0.11$  m. Then, having determined the values  $G_p$  and  $N_p$ , with the (33) we shall receive  $a_h = 0.0367$  m.

From the expression (26) it is possible to see, that the duration of the interferometer dynamic regime  $t_d$  will be defined by the tube of larger radius. As  $a_h > a_p$ , the value  $t_d$  will be defined by the value of "hydraulic" radius of the interferometer housing  $a_h$

$$t_d \approx 0.53 a_h^2 \nu^{-1}. \quad (36)$$

From the expression (36) it follows, that, having the measured values  $t_d$ , it is possible to determine the ether kinematic viscosity value

$$\nu \approx 0.53 a_h^2 t_d^{-1}. \quad (37)$$

The kinematic viscosity value, determined in such a way, we shall call as the ether kinematic viscosity measured value  $v_c$ . Let's substitute into (37) the values  $a_h = 0.0367$  m and the measured value  $t_d = (10 \dots 13)$  sec, we shall receive

$$\nu_c \approx (5.5 \dots 7.1) \cdot 10^{-5} \text{ m}^2 \text{ sec}^{-1}. \quad (38)$$

The kinematic viscosity mean value  $v_{ea}$ , calculated as the function mean value  $v = f(t_d)$  within  $(10 \dots 13)$  sec is equal to

$$\nu_{ea} = 6.24 \cdot 10^{-5} \text{ m}^2 \text{ sec}^{-1}. \quad (39)$$

Comparing (30), (38) and (39) we shall mark, that on the value order the ether kinematic viscosity values, calculated and measured, coincide  $v_c \approx v_e \approx v_{ea}$ .

The opportunity of the problem solution about the ether viscosity measuring is of particular interest, as the experimental data about the ether viscosity and the ether viscosity measuring methods miss in literature till nowadays.

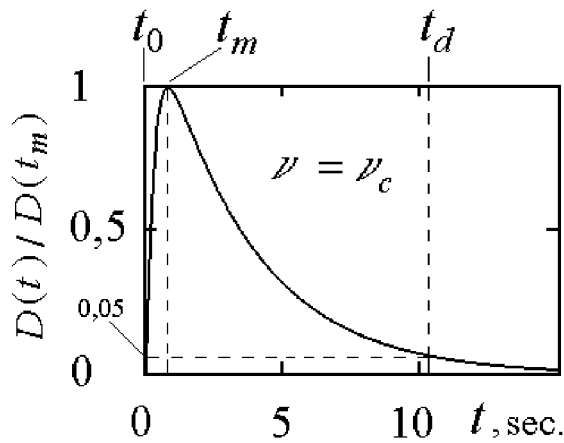


Figure 7: Variation in time of the interference pattern bands offset (calculation)

Let's write down the expression for the value  $D(t)$ . For this purpose we shall substitute the expressions (11) and (34) in (32) for the values  $w_p(t)$  and  $W_c(t)$  accordingly and, allowing the proportions (31), (35), we shall receive

$$D(t) \approx \pm \frac{8l_p W_h}{\lambda c} \sum_{k=1}^{\infty} \psi_k^{-3} J_1^{-1}(\psi_k) \cdot [\exp(-\nu \psi_k^2 a_p^{-2} t) - \exp(-\nu \psi_k^2 a_h^{-2} t)]. \quad (40)$$

In the Fig. 7 in a normalized view the dependence calculation result  $D(t)$ , performed with the expression (40) is given. At calculations the terms number of a series  $k = 4$ , the calculated value of the ether kinematic viscosity is  $\nu_c = 7 \cdot 10^{-5} \text{ m}^2 \text{ sec}^{-1}$  and the following values of the interferometer design parameters are used:  $a_p = 0.0105 \text{ m}$ ;  $a_h = 0.0367 \text{ m}$ ;  $l_p = 0.48 \text{ m}$ ;  $\lambda = 6.5 \cdot 10^{-7} \text{ m}$ .

From the Fig. 7 it follows, that on time expiration  $t_m \approx 0.82 \text{ sec}$ , which is digitized from the moment  $t_0$  of the beginning time of the interferometer dynamic operating regime, the bands offset maximal value of the interference pattern (value  $D$ ) should be observed. The anticipated duration of the interferometer dynamic operating regime matters  $t_d \approx 10.3 \text{ sec}$ . Let's use the expression (40) for specifying the observed value experimentally  $t_m \approx 1 \text{ sec}$ . For this purpose we shall substitute in (40) the measured value of the ether kinematic viscosity,  $\nu_{ea} = 6.24 \cdot 10^{-5} \text{ m}^2 \text{ sec}^{-1}$ , we shall receive  $t_m \approx 0.93 \text{ sec}$ . Hence, the calculation results do not contradict the experience results, which are shown in the Fig. 6.

The interferometer test results analysis, the ether kinematic viscosity values, calculated and measured, give the basis to consider, that the ether stream properties are close to the stream properties of known gases at their interaction with solids — to pass aside obstacles

and go in directing systems. It can be suspected, that solids (dielectrics, metals etc.) at interaction with the ether stream render major ether-dynamic resistance. It clarifies the interferometer test results, that the tube made of dielectric can execute the same directing system role for the ether, as the tube made of metal. The ether stream property, i.e. to pass aside obstacles, could cause unsuccessful attempts to detect the ether drift with the devices placed in metallic chambers [17-20, 23-26].

For value definition of the ether drift horizontal component velocity  $W_h$  it is possible to use the bands offset measured value of an interference pattern at the moment of time  $t_m$ , when  $D(t_m) = \max$ . From the expression (40) we shall receive

$$W_h \approx D(t_m) \lambda c \left\{ 8l_p \sum_{k=1}^{\infty} \psi_k^{-3} J_1^{-1}(\psi_k) \cdot [\exp(-\nu \psi_k^2 a_p^{-2} t_m) - \exp(-\nu \psi_k^2 a_h^{-2} t_m)] \right\}^{-1}. \quad (41)$$

Let's substitute in (41) the measured values of the ether kinematic viscosity  $\nu_{ea} = 6.24 \cdot 10^{-5} \text{ m}^2 \text{ sec}^{-1}$ , the value  $t_m = 1 \text{ sec}$ , the design parameters value of the interferometer and calculation parameter (the terms number of a series):  $a_p = 0.0105 \text{ m}$ ;  $a_h = 0.0367 \text{ m}$ ;  $l_p = 0.48 \text{ m}$ ;  $\lambda = 6.5 \cdot 10^{-7} \text{ m}$ ;  $k = 4$ . In this case the measured value of the ether drift horizontal component velocity, will be defined as follows

$$W_h \approx 525 D(t_m). \quad (42)$$

Let's calculate the minimal value of the ether drift velocity  $W_{hmin}$ , which can be measured with the manufactured interferometer, i.e. we shall determine the instrument sensitiveness. In the part "the interferometer test" is marked, that the minimum value  $D_{min}$ , which can be digitized with the selected eyefragment and scale  $D_{min} = 0.05$ . Then with the expression (42) we shall receive  $W_{hmin} = 26.25 \text{ m/sec}$ .

Let's determine the ether stream regime in the interferometer tubes at  $W_h = W_{hmin}$ . For this purpose with the expression (4) we shall calculate the minimal value of the Reynolds number  $Re_{min}$  for the tube with radius  $a_p = 0.0105 \text{ m}$ , in which the ether with the viscosity  $\nu_{ea} = 6.24 \cdot 10^{-5} \text{ m}^2 \text{ sec}^{-1}$  moves. Let's receive  $Re_{min} \approx 8834$ . According to the requirement (3) it can be written down, that  $Re_{min} > Re_c$ . Hence, at the ether drift velocities  $W_h \geq 26.25 \text{ m/sec}$  the ether stream turbulent regime is possible only in the interferometer tubes.

The optical interferometer tests and tests results analysis give the basis to consider, that the hydrodynamic description of the interferometer operating principle, reviewed above, is adequate to the imaginations about viscous ether stream in tubes, and the manufactured interferometer is suitable for the ether drift velocity and the ether kinematic viscosity measuring.

**The measurement methods.** The interferometer was disposed in the country settlement at the height ( $\approx 190$  m above sea level), in 13 km from Kharkov northern suburb. The proximate height ( $\approx 200$  m above sea level) is located westward apart 1.7 km. Two points were arranged for measurements. The distance between them was about 15 m. On the point No 1 the interferometer was at the height 1.6 m above the ground surface. On the point No 2 it was at the height 4.75 m. Two points available, which are located at different heights and are practically at the same point of terrain, it is required for observation of the "height effect." The measurements on the points No 1 and No 2 were performed in the open air. On the point No 1 the interferometer was in surrounding trees shadow and was not exposed to direct solar radiation affecting within a light day. On the point No 2 the interferometer was mounted in an umbrella shadow. In winter time the interferometer was transferred to Kharkov. The point No 3 ( $\approx 30$  m above the ground surface or  $\approx 130$  m above sea level) was arranged in the upper level facility of a bricky house. On the point No 1 the measurements were carried out in August 2001, on the point No 2 in August, September, October and November 2001, on the point No 3 in December 2001 and in January 2002.

The measurements were carried out cyclically. One measuring cycle lasted 25-26 hours. 2-4 cycles were performed within one month. Each cycle contained the following parameters. The interferometer was mounted on a selected point, so that its rotating plain was horizontal. After installation the interferometer was kept in new heating environment within one hour (the instrument was stored in the facility). The measurements were carried out at each whole hour of stellar time. One readout of the measured value was performed under the following schema. The interferometer longitudinal axis was mounted along a meridian, so that its illuminator was turned to the north. The further procedures did not differ from the interferometer operating procedures, which were applied at the final stage of the interferometer test. After the interferometer dynamic regime termination the observer registered the maximal bands offset value  $D(t_m)$ , as the measured value. The bands release time to their original position was registered and metered. The interferometer returned to the steady operating regime. The instrument turned to the initial position. As a rule, 5-7 readouts were done during one measuring time ( $\approx 10$  minutes). The readout mean value was accepted for the measured value  $D(S)$ , where  $S$  is the measuring stellar time.

**The processing methods of the measurement results.** The measurement results processing included the following procedures: values calculations of the ether drift horizontal component velocity  $W_h$ ; a daily course of the ether drift velocity within separate stellar day and the ether drift velocity daily course averaged during the year epoch  $W_h(S)$ ; a daily course of the

ether drift velocity averaged for the whole time of the measurement series  $\overline{W_h(S)}$ , mean-square value deflection  $W_h$  from its mean value  $\sigma_W$ .

The measurement results were introduced as the measured value tables  $D(S)$ . The values  $W_h$ , calculated with the expression (42) were brought to the same table for each hour of stellar day. Such numbers consequence obtained for separate stellar day, describes a daily course  $W_h(S)$ .

The mean values of the ether drift velocity and the values  $\sigma_W$  were calculated for each hour of the stellar day with the following known expressions [30]

$$\overline{W_h(S)} = \rho^{-1} \sum_{j=1}^{\rho} W_{hj}(S), \quad (43)$$

$$\sigma_W(S) = \left\{ \rho^{-1} \sum_{j=1}^{\rho} [W_{hj}(S) - \overline{W_h(S)}]^2 \right\}^{1/2}, \quad (44)$$

where  $\rho$  is the values amount  $W_h$ , obtained during the whole measurement series. The confidence intervals of the measured values were calculated with the known methods explained, for example, in the work [30]. The calculations were performed with the estimation reliability equal to 0.95.

**The measurement results.** The measurement series results, held since August 2001 till January 2002 are presented in the work. 2322 readouts of the measured values have been performed during this series. The distribution of readouts amount per months of the year is shown in the table 1

According to the research problems, we shall consider this work results along with the experiment results [1-3], [7-9], [10]. These four experiments have been performed at various points of a globe with three different measuring methods: an optical interferometer of the first order (Europe, Ukraine, 2001-2002 [this work]); a radio interferometer of the first order, (Europe, Ukraine, 1998-1999 [1-3]); optical interferometers of the second order (Northern America, USA, 1925-1926 [7-9], 1929 [10]). The measuring methods action, which are applied in the above-mentioned experiments, based on wave propagation regularities in moving medium, responsible for these waves propagation, that allows to treat the experiment results in the terms of the ether drift velocity within the original hypothesis.

The development regularities of viscous medium streams (fluids or gases) in directing systems are used in the work measuring method. The measured value is proportional to a velocity differential of the ether viscous streams in two tubes of different section within the original hypothesis. This differential value is proportional to the ether drift velocity (the first order method).

In the experiment measuring method [1-3] the regularities of viscous medium streams near the surface

Table 1: Distribution of readouts amount per months of the year

Month of the year	August 2001	September 2001	October 2001	November 2001	December 2001	January 2002
Amount of readouts	792	462	288	312	240	228

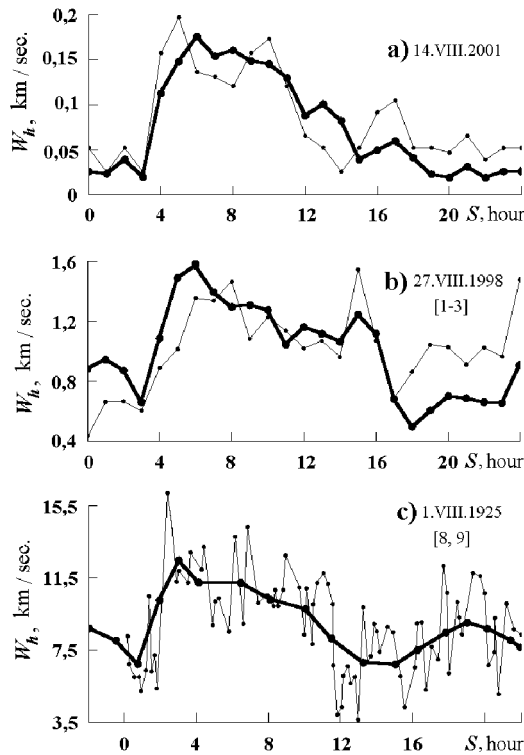


Figure 8: Variation of ether drift velocity within a day in August epoch

partition are used. The measured value is proportional to a vertical velocity gradient in the ether drift stream near the Earth's surface within the original hypothesis. This gradient value is proportional to the ether drift velocity (the first order method).

In the experiments [7-9] and [10] Michelson's cruciform interferometers were applied. The measured value is proportional to a velocity differential of wave propagation in orthogonal related directions in the ether drift stream within the original hypothesis. This differential value is proportional to the ether drift velocity (the second order method).

In the Fig. 8 the experiment results referring to August are presented. On fragments of this figure are shown accordingly: in the Fig. 8a — this work results; in the Fig. 8b — the experiment results [1-3] (the figure is published for the first time); in the Fig. 8c — the experiment results [7-9].

The ether drift velocities  $W_h$  in km/sec. are pending on ordinate axes. The stellar time  $S$  in hours is

pending on abscissa axes. Each of the Fig. 8 fragments illustrate the variation of the ether drift velocity within a stellar day  $W_h(S)$ . The experiment results are presented only by the authors of work [10] as ascertaining of the velocity maximal value, measured by them, in relation to the movement  $W \approx 6$  km/sec, that has not allowed to show this experiment results in the Fig. 8 as the daily dependence  $W_h(S)$ . In the Fig. 8 the measurement data averaging results were presented with the thick lines, which are obtained in each of the experiments during August epoch (mean results). The separate observations (measurement results during a separate day) are shown with thin lines. The dates of separate observations are specified on fragments. The separate observations on fragments of the Fig. 8a, Fig. 8b are selected from the performings, which had the date, proximate to the date of separate observation of the Fig. 8c fragment and which during the day had no skips during the measuring. The date discrepancy is stipulated also by the fact that the systematic measurements in the work began on August 14, 2001, and in the experiment [1-3] — on August 11, 1998.

The positive measurement results, given in the Fig. 8, illustrate the development of anisotropy effect — the ether drift required effect. In the work and in the experiments [7-9], [10] the anisotropy effect was discovered by the optical interferometer rotation, in the experiment [1-3] the opposing radio waves propagation was applied.

The similar nature of the ether drift velocity variation within a day in August epoch unite all three fragments of the Fig. 8. The first minimums in dependencies  $W_h(S)$  are expressed clearly in all three mean results. In the work (Fig. 8a) and in the experiment [1-3] (Fig. 8b) temporary position of minimums is  $S \approx 3$  hours. In the experiment [7-9] (Fig. 8c) the temporary position of the first minimum is  $S \approx 0.8$  hour. (Such discrepancy in the position of these minimums is about 2.2 hour, an explanation has not found yet.) The ether drift velocity magnification is observed during consequent 2-3 hours. Further the plateau sites with rather small variations of the ether drift velocity in time are noticed on all fragments. The greatest duration of the plateau site was observed in the experiment [1-3] (Fig. 8b), that can be explained by arranging peculiarities of a radio-frequency spectral line on terrain. In this experiment the radio-frequency spectral line is declined from a meridian on  $45^\circ$  to northeast. The variations

of the ether drift apex azimuth (as well as any star azimuth) occur symmetrically to a meridian line within a stellar day. If to take the apex coordinate values into account (according to Miller:  $\delta \approx 65^\circ$ ,  $a \approx 17.5^h$  [9]), the ether drift azimuth in this part of a stellar day accepts the values, which lay in the northeast direction, i.e. in the direction close to the direction of a radio-frequency spectral line. In this case the angle between the ether drift azimuth and radio frequency spectral line direction has minimum values. Accordingly at the interval of 12-16 hours the ether drift radial component velocity (directed along a radio-frequency spectral line) keeps rather high value, despite of the apex height magnification (astronomical coordinate). Such arranging peculiarities of the radio interferometer on terrain can explain the relative dependence increase  $W_h(S)$  at the interval of 12-16 hours in comparison with the same dependencies shown on two other fragments. In the work (Fig.8a), according to the accepted measurement methods, the optical interferometer was located along a meridian. As the variations of the ether drift azimuth within a stellar day occur symmetrically to the meridian line, in this case the plateau site duration should be less, than in the experiment [1-3] and less than in the experiment [7-9] in which the ether drift azimuth variation was considered by the corresponding rotation of the interferometer.

It can be seen in the Fig. 8a (the mean result of the work), that the sites with rather small values of the ether drift velocity, extended in time, take place within a day. Noticeable bands offset of an interference pattern was not observed per a separate day on such sites. In these cases the ether drift velocity was lower than the interferometer sensitiveness (i.e.  $W_h < 26$  m/sec), that was used for the interferometer tests, the purpose of which is given in the above mentioned part "the interferometer test".

Systematic character of experimental investigations of this work and the works [1-3], [7-9] has shown, that dependencies measured in one and the same epoch of the year  $W_h(S)$ , have the similar character of the ether drift velocity variation within a day. At the same time dependencies view  $W_h(S)$ , measured in different epochs of the year differ from each other, that can be noticed, for example, by the experiment published results [7-9]. The reasons of such seasonal variations have not been defined yet. It can be suspected, that magnetosphere, at its considerable sizes and peculiar shape, ionosphere, the known variations of their state can be responsible for such dependence variations  $W_h(S)$ .

It can be seen in the Fig. 8, the ether drift velocities, measured in each of the experiments, differ, that can be stipulated by the arranging height differences of measuring systems above the Earth's surface: 1.6 m; 42 m; 1830 m (Fig. 8a, Fig. 8b, Fig. 8c accordingly). The collection of such data illustrates the height effect development. In the work the ether drift velocity mea-

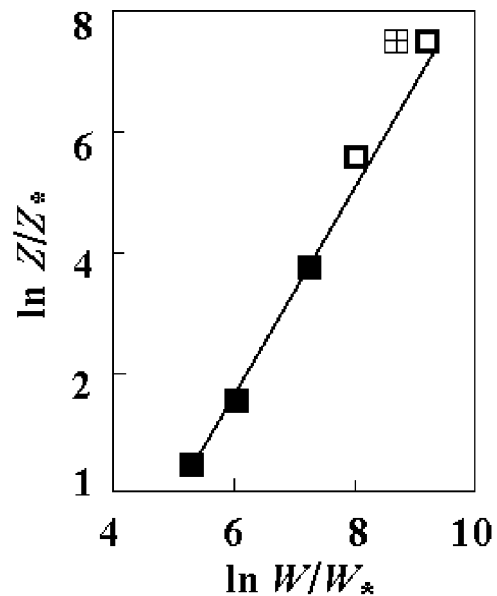


Figure 9: Dependence of the ether drift velocity on the height above the Earth's surface, ■ is this work and experiment [1-3]; □ is the experiment [7-9]; ⊠ is the experiment [10]

suring have been performed at the heights 1.6 m and 4.75 m (position No. 1 and No. 2) for height dependence discovery. In the table 2 the mean values of the ether drift maximal velocity are given, which are measured in the work and in the experiments [1-3], [7-8], [10]. In these four experiments the measurements are performed at five different heights: 1.6m and 4.75 m in the work; 42 m in the experiment [1-3]; 265 m and 1830 m in the experiment [7-9] (Cleveland and the observatory of Mount Wilson accordingly). In the experiment [10] the measurements were carried out also on the observatory of Mount Wilson. However, in contrast with the experiment [7-9], which was carried out in a light wooden house, the experiment [10] is performed in a fundamental building of an optical workshop of the observatory. It can be supposed, that the ether stream braking by the house walls was the reason of the ether drift velocity smaller value, measured in the experiment [10] in comparison with the experiment result [7-9].

The table 2 gives the imagination about the ether drift velocity variation in height band above the Earth's surface from 1.6 m up to 1830 m. In the figure 9 this dependence view is presented in the logarithmic scale. On the abscissa and ordinates axes the logarithmic values of ratios  $W/W_*$  and  $Z/Z_*$  were pending accordingly, where:  $W$  is the ether drift velocity at the height  $Z$ ; the values  $W_*$  and  $Z_*$  are considered equal to 1 m/sec and 1 m accordingly.

Table 2: Dependence of the ether drift velocity on the height above the Earth's surface

Height above the Earth's surface (meters)	The ether drift velocity (m/sec)			
	This work 2001-2002 Optics	The experiment [13] 1998-1999 Radio waves band	The experiment [79] 1925-1926 Optics	The experiment [10] 1929 Optics
1830	–	–	10000	6000
265	–	–	3000	–
42	–	1414	–	–
4.75	435	–	–	–
1.6	205	–	–	–

It can be seen from the Fig. 9, that different experiment results are near one straight line and in height band from 1.6 m up to 1830 m the ether drift velocity increases with the height growth above the Earth's surface. The boundary layer has considerable thickness, that can be the consequence of the ether stream and atmosphere interaction. These data do not contradict the imaginations of the model [4-6] about the viscous ether and its stream near the Earth's surface. From the table 2, Fig. 8a and the Fig. 9 it can be seen, that the ether drift velocity is rather small near the Earth's surface, that can explain the reason of "zero results" of many experimental works, in which the value 30 km/sec was taken as the ether drift anticipated velocity. In such experiments the metering device sensitiveness was obviously poor. With the expression (1) it can be calculated, that at the ether drift velocity 200-400 m/sec, the methods of the second order almost are inapplicable for measurements, as in this case such methods sensitiveness to the ether drift velocity is low in 6 orders (!) than the sensitiveness of the first order methods.

The ether kinematic viscosity has been measured in the work. The measurement results are explained above in the part "Result analysis of the interferometer tests," that is stipulated by the peculiarities of the experiment implementation. The measured values of the ether kinematic viscosity are in the limits  $v_{ea} \approx (5.5 \dots 7.1) \cdot 10^{-5} \text{ m}^2\text{sec}^{-1}$ . The mean value is equal  $v_{ea} = 6.24 \cdot 10^{-5} \text{ m}^2\text{sec}^{-1}$ , that according to the value order coincides with the ether kinematic viscosity value calculated above  $v_c \leq 7.06 \cdot 10^{-5} \text{ m}^2\text{sec}^{-1}$ .

Hence, the differences between the dependencies  $W_h(S)$  and the ether drift velocity measured values available can be explained by the measurement method differences of the work and the experiments [1-3], [7-9], [10] and differences between arranging heights of measuring systems. The results of four experiments do not contradict each other, that illustrate the reproduced measurement nature of the ether drift effects in various experiments performed in different geographic conditions with different measurement methods applying.

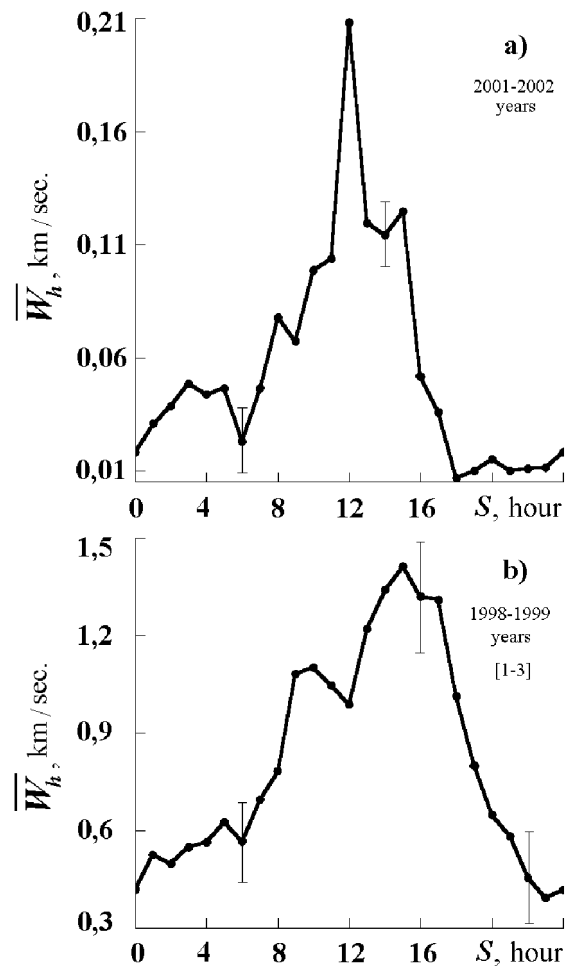


Figure 10: The mean daily course of the ether drift velocity



According to the original hypothesis, the ether drift velocity horizontal component  $W_h$  should change its value with the period per one stellar day (the space effect). For revealing the ether drift velocity component with such period, the results of systematic measurements were subjected to statistical processing in stellar time scale. The results of such processing are shown in the Fig. 10. On the fragments of the Fig. 10 the stellar time  $S$  in hours is suspended on the abscissa axes, the ether drift velocity value  $W_h$  in km/sec is suspended on the ordinate axes. The vertical hatches indicate the confidence intervals. In the Fig. 10a the mean daily course of the ether drift velocity within a stellar day  $\overline{W_h}(S)$  is given. This dependence is calculated according to the measurement results of the work, which were performed during five months of the year, since September 2001 till January 2002. During five months the numerical value of stellar time shifts regarding to the solar time in 10 hours. Since September till November the measurements were performed on the point No2. In December and January — on the point No3. The mean values are calculated with the expression (43). For comparison, in the Fig. 10b the mean result is given, which was obtained in the experiment [1-3] during year's five months of the same name, since September 1998 till January 1999 (Here, as contrasted to the similar figure, given in the works [1-3], the measured value is expressed in the ether drift velocity values.) In the works [7-9], [10] such data miss, owing to smaller on coverage of year's epochs of the measurement statistics in these experiments.

Both fragments of the Fig. 10 as a whole have similar nature of the ether drift velocity variation within a day. The differences in the curve shapes can be explained by viscous ether stream interaction with the terrain relief elements, which in these different experiments had the distinguished performances and features of radio-frequency spectral line arranging on terrain in the experiment [1-3]. On the fragment of the Fig. 10a (this work), as contrasted to the result of the experiment [1-3] (Fig. 10b), the ether drift velocities have smaller values, that can be explained by the height distinction of measuring points in these experiments. The dependencies  $\overline{W_h}(S)$  have the forms of periodically changed values with the periods equal to a stellar day, that can be explained by a space (galactic) origin of the ether drift. In the work, the observed bands offset direction of an interference pattern corresponded to the ether drift northern direction at measurement implementation. Hence, the results of the work do not contradict the experiment results [1-3], [7-9], [10] and imaginations of the works [4-6] about the northern position of the ether drift apex, that demonstrate the reproduced result nature of the ether drift effects measurement in different experiments, performed with different measuring methods application.

In the work we shall be confined to qualitative comparison of the work results with the experiment data [1-3], [7-9], [10]. For conducting of quantitative comparative analysis it is necessary to specify the ether drift apex coordinate values on the celestial sphere, which for the first time were determined in the experiment [7-9], to specify an analytical view of the ether drift velocity dependence on the height above the Earth's surface proposed in the works [1-3], to elaborate the calculation method of the terrain relief influence on the ether streams forming near the Earth's surface, to determine probable influencing of the Earth magnetosphere and ionosphere, that is the subject of separate investigations and goes out the frame of the work problems. Due to the reason this experiment results, the experiment [1-3] and the experiment [7-9] are given without any correction, though its usefulness at the result comparison of different experiments is quite obvious.

Thus, in the work, the hypothesis experimental verification about the ether existence in nature, i.e. material medium, responsible for electromagnetic waves propagation, in the optical wave band has been performed. The estimation of the ether kinematic viscosity value has been performed. The first order optical method for the ether drift velocity and the ether kinematic viscosity measuring has been proposed and realized. The method action is based on the development regularities of viscous liquid or gas streams in the directing systems. The significant measurement results have been obtained statistically. The development of the ether drift required effects has been shown. The measured value of the ether kinematic viscosity on the value order has coincided with its calculated value. The velocity of optical wave propagation depends on the radiation direction and increases with height growth above the Earth's surface. The velocity of optical wave propagation changes its value with a period per one stellar day. The detected effects can be explained by the following:

- optical wave propagation medium available regarding to the Earth's movement;
- optical wave propagation medium has the viscosity, i.e. the feature proper to material mediums composed of separate particles;
- the medium stream of optical wave propagation has got a space (galactic) origin.

The work results comparison to the experiment results, executed earlier in order of the hypothesis verification about the existence of such material medium as the ether in nature, has been performed. The comparison results have shown the reproduced nature of the ether drift effect measurements in various experiments performed in different geographic requirements with different measurement methods application.

The work results can be considered as experimental hypothesis confirmation about the ether existence in nature, i.e. material medium, responsible for electromagnetic waves propagation.

## References

- [1] Yu. M. Galaev. "Ether-drift effects in the experiments on radio wave propagation." *Radiophysics and electronics*, 2000, Vol. 5, No.1, pp. 119–132. (in Ukraine).
- [2] Yu. M. Galaev. "Ether-drift. Experiment in the band of radio wave." Zhukovskiy: Petit, 2000, 44 pp. (in Russia).
- [3] Yu. M. Galaev. "Etheral wind in experience of millimetric radiowaves propagation." *Spacetime & Substance*, 2001, Vol. 2, No. 5(10), pp. 211–225, <http://www.spacetime.narod.ru/0010-pdf.zip>.
- [4] W. Azjukowski. "Dynamik des Äthers." *Ideen des exakten Wissens.*, Stuttgart, 1974, Nu. 2, s. 48–58.
- [5] V.A. Atsukovsky. "The introduction into etherdynamics. Model imaginations of material and field structures on the basis of gas like ether." Moscow, MOIP physics dep., 1980, Dep. in VINITI 12.06.80 No. 2760-80 DEP. (in Russia).
- [6] V.A. Atsukovsky. "General ether-dynamics. Simulation of the matter structures and fields on the basis of the ideas about the gas-like ether." Energoatomizdat, Moscow, 1990, 280 pp. (in Russia).
- [7] D.C. Miller. "Ether drift experiments at Mount Wilson solar observatory." *Phys. Rev.*, 1922, Vol. 19, pp. 407–408.
- [8] D.C. Miller. "Ether drift experiment at Mount Wilson." *Proc. Nat. Acad. Amer.*, 1925, Vol. 11, pp. 306–314.
- [9] D.C. Miller. "Significance of the ether-drift experiments of 1925 at Mount Wilson." *Science.*, 1926, Vol. 68, No. 1635, pp. 433–443.
- [10] A.A. Michelson, F.G. Pease, F. Pearson. "Repetition of the Michelson-Morley experiment." *Journal of the Optical Society of America and Review of Scientific Instruments.*, 1929, Vol. 18, No. 3, pp. 181–182.
- [11] E.T. Whittaker. "A History of the Theories of Aether and Electricity." Izhevsk: RIC Regular and random dynamics, 2001, 512 pp. (in Russia). E.T. Whittaker. "A History of the Theories of Aether and Electricity." Thomas Nelson and Sons Ltd, Edinburgh, 1953.
- [12] A.A. Michelson. "The relative motion of the Earth and the Luminiferous ether." *The American Journal of Science.*, 1881, III series, Vol. 22, No. 128, pp.120–129.
- [13] G.G. Petrash, S.G. Rautian. "Michelson's Interferometer." In the book "Physical encyclopaedic vocabulary." The Soviet encyclopedia, Moscow, 1962, Vol. 2, pp. 202–203 (in Russia).
- [14] A.A. Michelson, E.W. Morley. "The relative motion of the Earth and the luminiferous aether." *The American Journal of Science. Third Series.*, 1887, Vol. 34, pp. 333–345; *Philosophical journal.*, 1887, Vol. 24, pp. 449–463.
- [15] W.I. Frankfurt, A.M. Frank. "Optics of moving media." Nauka, Moscow, 1972, 212 pp. (in Russia).
- [16] S.I. Vavilov. "New searches of "the ether drift"." *Successes of physical sciences*, 1926, Vol. 6, pp. 242–254 (in Russia).
- [17] R.J. Kennedy. "A refinement of the Michelson-Morley experiment." *Proc. Nat. Acad. Sci. of USA.*, 1926, Vol. 12, pp. 621–629.
- [18] K.K. Illingworth. "A repetition of the Michelson-Morley experiment using Kennedy's refinement." *Physical Review.*, 1927, Vol. 30, pp. 692–696.
- [19] E. Stahel. "Das Michelson-Experiment, ausgefuhrt im Freiballon." "Die Naturwissenschaften," Heft 41, 1926, B8, Nu. 10, S. 935–936.
- [20] Joos G. Die Jenaer. "Widerholung des Mihelsonversuchs." *Ann. Phys.*, 1930, B7, S. 385–407.
- [21] "Ether-drift," Digest by Dr. in Sc. V.A. Atsukovsky. Energoatomizdat, Moskow, 1993, 289 pp. (in Russia).
- [22] D.C. Miller. "The ether-drift experiment and the determination of the absolute motion of the Earth." *Rev. Modern. Phys.*, 1933, Vol. 5, No. 3, pp. 203–242.
- [23] L. Essen. "A new ether drift experiment." *Nature.*, 1955, Vol. 175, pp. 793–794.
- [24] J.P. Cedarholm, G.F. Bland, B.L. Havens, C.H. Townes. "New experimental test of special relativity." *Phys. Rev. Letters.*, 1958, Vol. 1, No. 9, pp. 342–349.
- [25] D.C. Cyampney, G.P. Isaac, M. Khan. "An ether drift experiment based on the Mssbauer effect." *Phys., Letters.*, 1963, Vol. 7, pp. 241–243.
- [26] T.S. Jaseja, A. Javan, J. Murbeam, C.H. Townes. "Test of special relativity or space isotropy by use of infrared masers." *Phys. Rev.*, 1964. Vol. 133a, pp. 1221–1225.
- [27] L.G. Loytsyansky. "Mechanics of fluid and gas." Nauka, Moscow, 1973, 848 pp. (in Russia).
- [28] N.A. Slezkin. "Dynamics of viscous incompressible fluid." Gostechizdat, Moskow, 1955, 520 pp. (in Russia).
- [29] S.G. Rautian. "Rozhdestvensky's Interferometer." In the book "Physical encyclopaedic vocabulary." The Soviet encyclopedia, Moscow, 1962, Vol. 2. p. 203 (in Russia).
- [30] L.Z. Rumshisky. "Mathematical processing of the experiment results." Nauka, Moscow, 1971, 192 pp. (in Russia).